FRET between CdSe Quantum Dots in Lipid Vesicles and Water- and Lipid-soluble Dyes

Jeremiah A. Kloepfer,[†] Netta Cohen,[‡] and Jay L. Nadeau*[,†]

Jet Propulsion Laboratory, California Institute of Technology, Pasadena, California 91109, and School of Computing, University of Leeds, Leeds LS2 9JT, U.K.

Received: May 3, 2004; In Final Form: July 9, 2004

Because of the coatings needed to solubilize and passivate quantum dots for biological applications, their use in fluorescent resonance energy transfer (FRET) has been limited. However, hydrophobic particles without polymer coatings may be embedded into lipid membranes, as demonstrated here with biomimetic vesicles. FRET is seen to a lipid-soluble dye (DiD) and a water-soluble dye (Cy3.5) in which the vesicles are suspended. The degree of energy transfer to each dye suggests that most of the QDs are located deep within the lipid, as confirmed by electron microscopy of whole mounts and thin sections of vesicles. Energy transfer is also seen to a voltage-sensitive, lipid-soluble dye (di-4-ANEPPS) only when the potassium ionophore valinomycin is present in the membrane. The effect is dependent upon potassium ion concentration rather than absolute membrane potential.

Introduction

The spectral properties of semiconductor quantum dots (QDs) make them ideal fluorescence resonance energy transfer (FRET) donors. For FRET to occur, the emission spectrum of a donor fluorophore must overlap the absorbance spectrum of an acceptor; with their broad absorbance and narrow emission, QDs have the promise to allow FRET with minimal donor−acceptor spectral overlap. However, the energy transfer is a dipole−dipole interaction and hence, drops off with distance between the pair as r^6. Biocompatible QDs are usually passivated by a polymer layer and a protein layer, creating stable, high-quantum-yield photoluminescence (PL) but increasing the particle size by up to 10 nm and reducing or eliminating FRET. To reduce this distance, researchers have coupled proteins directly to QDs, allowing energy transfer between the QDs and the protein tryptophan residues[1] or have coupled QDs to a genetically engineered myelin basic protein (MBP) whose tight binding to the QD surface results in a thin overlayer and energy transfer to a molecule outside the MBP.[2] FRET has also been demonstrated with protein-conjugated QDs as both acceptors and donors.[3]

However, biological phenomena are not restricted to those in water. The ability to label cell membranes is of great importance in studying vesicle trafficking, visualizing nerve terminals, understanding membrane fusion, and other applications.[4−7] In this article, we demonstrate that hydrophobic QDs can act as FRET donors, and possibly also as acceptors, within a model membrane system using biomimetic lipid vesicles. This is the first time that energy-transfer processes of unsolubilized QDs have been explored in a biological context. As well as demonstrating the possibility of FRET, these experiments also suggest that hydrophobic QDs can associate within lipid membranes without significant damage to the membrane such as increased leakage. Although the QDs are hydrophobic, FRET is seen to both a hydrophilic dye that is able to float free in solution around the membrane (Cy 3.5) and a hydrophobic dye that inserts into the lipid layer in a similar manner as the QDs (1,1′-dioctadecyl-3,3,3′,3′-tetramethylindodicarbocyanine, 4-chlorobenzenesulfonate, DiD). In the case of the hydrophilic dye, only partial FRET is seen; in the case of the lipophilic dye, FRET efficiencies can approach 100%.

The advantages of use of hydrophobic QDs are several. The quantum yield of the unsolubilized particles is much higher than in those rendered water soluble, and the particles themselves are more stable. In addition, many biological processes occur within lipid membranes, ones that are often poorly understood because of the difficulty in probing this 5-nm-thick hydrophobic interface. Their natural hydrophobicity makes QDs obvious candidates for sensing transmembrane or intermembrane processes, a key example of which is the transmembrane electrical potential. Particles embedded in a cell membrane experience any voltage drop that exists across that membrane; in certain types of cells, this voltage can be greater than 100 mV/10 nm (10^5 V/cm). This means that it may prove possible to exploit the semiconductor and/or FRET properties of the QDs to create a probe that changes intensity or emission spectrum with applied voltage.

Such a voltage-sensitive indicator remains an elusive holy grail of some branches of physiology. Currently existing organic voltage-sensitive dyes, which are lipophilic fluorophores that change spectrum according to the potential drop across a lipid bilayer, are used to measure activity in neurons and cardiac cells.[8] Their usefulness is greatly limited by the small size of their spectral changes with voltage and the lack of quantitative understanding of their properties.[9] In this article, we test the possible utility of QDs as voltage-sensitive probes in two ways. The model system makes use of the same biomimetic vesicles as in the experiments using DiD and Cy 3.5; a Nernst potential is generated across the vesicle bilayer by varying the concentrations of K^+ ions internal and external to the vesicles and creating charge separation using a pore-forming peptide that is selective for K^+ (valinomycin).

QDs themselves, in this model system, show insignificant spectral shifts with voltage, indicating that features of the semiconductor particles such as the Stark shift are too small to

* Corresponding author. Current address: Department of Biomedical Engineering, McGill University, 3775 University St., Montreal QC Canada H3A 2B4 Phone: 514-398-8372. Fax: 514-398-7461. E-mail: jay.nadeau@mcgill.ca.

[†] California Institute of Technology.

[‡] University of Leeds.

10.1021/jp048094c CCC: $27.50
Published on Web 10/09/2004

be measurable here. The second approach we take is to embed both QDs and the most commonly used voltage-sensitive dye (3-(4-(2-(6-(dibutylamino)-2-naphthyl)-*trans*-ethenyl)pyridinium)propanesulfonate [di-4-ANEPPS]) into the same vesicles. Very large shifts in emission spectra are seen upon addition of valinomycin, and the results depend strongly upon K^+ concentration. Interpretation of results is difficult due to the extremely broad absorption and emission spectra of di-4-ANEPPS; however, the shifts seen appear to result from direct interactions between K^+, ANEPPS, and QDs rather than from the absolute value of the Nernst potential. The implications of these results for eventual use of QDs in voltage-sensitive applications are discussed.

Experimental Section

QDs in this study were synthesized as previously described.[10,11] To form the ZnS shell,[12] the hot reaction mixture was allowed to cool to ~180 °C and 5 mL of ZnS precursor (hexamethyldisilathiane and dimethylzinc in trioctylphosphine (TOP) was added dropwise over the course of 10 to 15 min and baked for 1−2 h. Resulting QDs were washed several times in methanol and dissolved in CH_2Cl_2. This yields CdSe/ZnS nanocrystallites passivated with trioctylphosphine oxide (TOPO). TOPO was removed by 2 washes in hexane/pyridine.[13] The fluorescence quantum yield was not changed significantly by TOPO removal. The quantum yield was measured at an excitation wavelength of 450 nm using a standard with a published value of 1 (rhodamine 101 in ethanol). The formula[14]

$$QY = QY_R \frac{I}{I_R} \frac{OD_R}{OD} \frac{n^2}{n_R^2} \quad (1)$$

was used where R refers to rhodamine and *n* refers to the indices of refraction of the respective solutions (1.424 for CH_2Cl_2 and 1.3605 for ethanol). Resulting values were 10% for green QDs, emission peak at 570 nm; 12% for red QDs, emission peak at 620 nm. The stock solutions had a concentration of ~1 μM based upon mean particle size (3.5 nm, determined by high-resolution electron microscopy) and an assumed extinction coefficient (10^5 cm^{-1} M^{-1}at the first exciton peak).[15]

To form vesicles with QDs, we added 10 μL of stock QD solution to 100 μL of the lipid 1,2-dioleoyl-*sn*-glycero-3-phosphocholine (DOPC) in chloroform (Avanti Polar Lipids no. 850375, Alabaster, AL). The solution was dried under N_2, suspended in 1 mL of buffer, and ultrasonicated until cloudy. The suspension was subjected to three rounds of freeze−thaw in liquid N_2, and the resulting vesicles were inspected by epifluorescence microscopy and transmission electron microscopy (TEM). An Akashi EM-002B microscope operating at 100 kV was used to for TEM and also for energy-dispersive X-ray spectroscopy (EDS). The area sampled by the Oxford spectrum analyzer is approximately 8.8 nm, and a wt % of >2% Cd or Se was taken to be significant. The acquisition rates were maintained at 10−20% deadtime with 60 s of livetime at 83 kX. The electron beam was defocused at the condenser lens to maintain counting rates below 1 kHz and live time efficiency >95%.

Vesicle preparations were visualized three ways: unstained, negative stained, and thin sectioned (to determine location of the particles within the membrane). The preparation of unstained mounts was performed by depositing 10−20 μL of fresh (collected within 2 h) vesicles in buffer onto carbon-coated Cu grids. After 2 min, the excess solvent was wicked away with filter paper, leaving behind vesicles deposited on the grid surface. After being allowed to air dry, the grids were washed 2−3 ×times in dH_2O to remove any traces of buffer. Negatively stained preparations were prepared by staining the grid with 2% uranyl acetate for 30 s after the sample was dry. To prepare thin sections, the vesicles were sedimented by centrifugation (2 min at 14 000 rpm in a tabletop microcentrifuge) and the pellet was dispersed in Noble agar worms of desired length. The samples were stained by post fixing in osmium tetroxide and staining with uranyl acetate; they were then dehydrated in ethanol and acetone before being embedded in EPON resin. Sample resin blocks were trimmed and sectioned (50−60 nm) on an MT-X Ultramicrotome with a 45° Diatome diamond knife. Ultrathin sections were placed on 200-mesh Formvar/carbon-coated copper grids. The prestained ultrathin section samples were subsequently poststained with 2% uranyl acetate before final imaging.

Buffers used were "low K^+" 1 mM KCl, 0.2 mM EGTA, 20 mM HEPES, and sucrose, and "high K^+" 150 mM KCl, 5 mM EGTA, and 20 mM HEPES; the osmolarity was adjusted to within ±2 mOsm with sucrose. After the final round of freeze−thaw, the vesicles were diluted 1:10 into the appropriate buffer in a 96-well plate with 300 μL wells. Experiments using Cy 3.5 and DiD were performed using a low K^+ buffer inside and outside the vesicles; experiments using di-4-ANEPPS were performed at varying K_{in}/K_{out} (Results and Discussion). Emission spectra were taken on a Gemini EM plate reader in epifluorescence mode. Dyes were added to the wells as stock solutions: Cy3.5, 10 μM in buffer; DiD, 10 mg/mL in DMSO diluted to 0.1 mg/mL (~0.1 mM) in buffer, and di-4-ANEPPS, 2 mM in ethanol, diluted 0.1 μM in buffer. All dyes were added in 1 μL increments to the experimental wells (DiD control wells received diluted DMSO only, and ANEPPS controls received ethanol only). Controls for the lipid-soluble dyes were lipid vesicles containing no QDs. The Cy 3.5 used was conjugated to a DNA oligomer (22 base pairs in length), but is simply referred to as Cy 3.5 in this paper.

For voltage-dependence experiments using di-4-ANEPPS, spectra were collected with and without 1μM valinomycin in DMSO. Spectra were stable for at least 5 h after the addition of valinomycin. The spectra shown in the Results and Discussion section reflect an excitation wavelength of 440 nm; spectra were also taken at 360, 400, and 530 nm. The spectra at 360 and 530 nm are available in the Supporting Information. Absorbance spectra were recorded with a Hewlett-Packard 8453 UV−vis spectrophotometer. Excitation spectra were taken on a Gemini EM plate reader in excitation mode using much lower concentrations of QDs than were used for the absorbance spectra (optical density of solutions <0.05). This avoided artifacts but resulted in excitation spectra in which typical absorbance peaks could not be seen (Results and Discussion).

Results and Discussion

Spectra. Emission spectra of vesicle-embedded QDs were not changed from those of the original QDs, showing broad absorption to the band edge and narrow emission. Significant overlap was observed between the emission of green QDs and Cy 3.5 and of both red and green QDs and DiD (Figure 1A and B). With the voltage-sensitive dye di-4-ANEPPS, QDs may function as acceptors rather than donors (Figure 1C).

FRET to DiD and Cy3.5. No changes in emission spectrum were seen upon the addition of any dye to QDs in vesicles when the QDs remained passivated with trioctylphosphine oxide. In addition, even after the removal of this inorganic layer by pyridine wash, no quenching of QD emission was seen upon

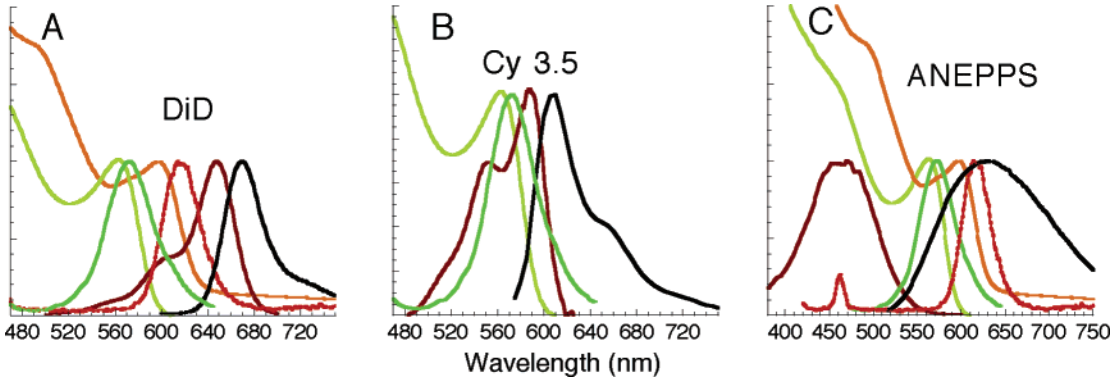

Figure 1. Absorbance (Abs) and emission (Em) spectra of green-emitting QDs (Abs: yellow-green, Em: green), red-emitting QDs (Abs: orange, Em: red) and dyes (Abs: maroon, Em: black). The *y* axes are arbitrary units. (A) Green-emitting QDs are able to function as donors to DiD, but not so efficiently as red QDs. (B) Only green-emitting QDs show spectral overlap with Cy 3.5. (C) The spectrum of di-4-ANEPPS at 0 transmembrane potential shows a potential role of QDs as acceptors but not donors. The vertical lines indicate the excitation wavelengths used in this study: 400, 440, and 530 nm (not shown but also tested was 360 nm). Shifts in spectrum due to the membrane potentials used in this study (±126 mV, Results and Discussion section) are not large enough to affect the overlap significantly (data not shown).

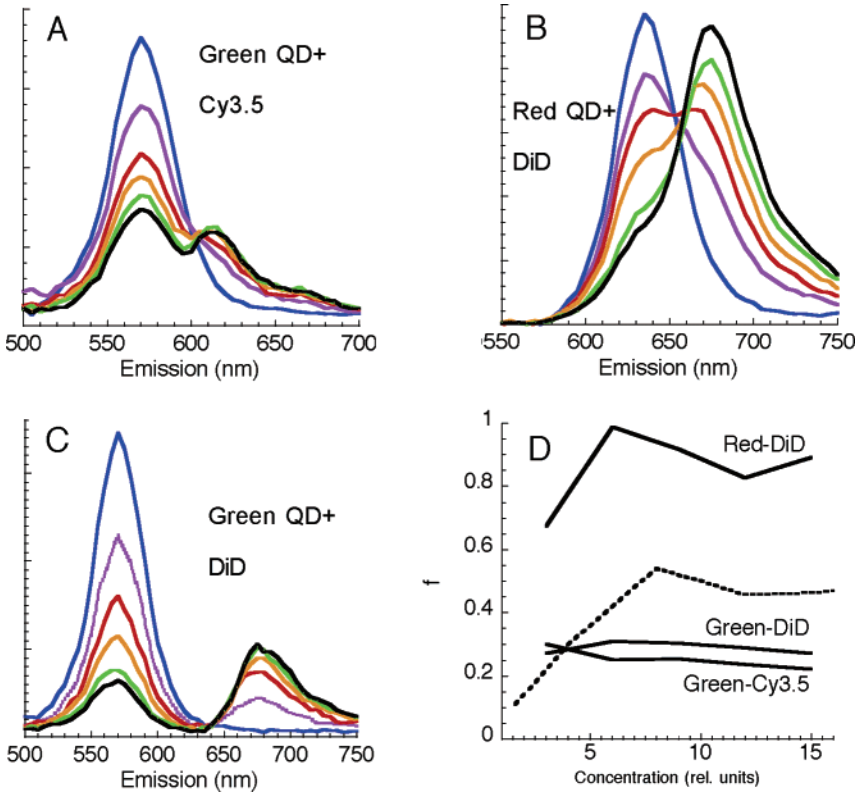

Figure 2. FRET between QDs in vesicles and dyes in lipid and in solution. Excitation = 400 nm. (A−C) Shown are emission spectra in arbitrary units for: QDs alone (blue), then after addition of 3 (violet), 6 (red), 9 (orange), 12 (green), and 15 (black) μL of a stock solution (10 μM Cy 3.5; 0.1 mM DiD). Background, represented by directly excited dye and vesicle scatter, was subtracted from all traces. (D) Fraction of QD quenching that is due to FRET (*f*, dimensionless) plotted against dye concentration in relative units. Shown are red QDs and DiD in vesicles (Red-DiD); green QDs and DiD in vesicles (Green-DiD); and green QD in vesicles with Cy3.5 in external solution (Green-Cy3.5). Shown for comparison (- - -) are values from another study in which QDs acted as donors to tetramethylrhodamine in solution.[17]

the addition of Cy3.5 to red QD vesicles, up to a concentration of 150 μM. With washed QDs, significant quenching of QD fluorescence and an associated increase in dye emission were seen with green QDs and Cy3.5 and with both red and green QDs and DiD (Figure 2A−C).

Using the formula

$$f = \frac{\phi I_{\mathrm{FRET}}^{\mathrm{dye}}}{f I_{\mathrm{quench}}^{\mathrm{QD}}} \frac{\phi^{\mathrm{QD}}}{\phi^{\mathrm{dye}}} \qquad (2)$$

yields values of fluorescence quenching due to FRET of 22−30% for green QD−Cy3.5, from 27−31% for green QD−DiD, and from 67−98% for red QD−DiD across the dye concentration ranges, using a recently published value of 12% for the quantum yield of DiD in lipid,[16] and a value for Cy 3.5 of 15% (Figure 2D). These data imply highly efficient energy transfer between the QDs and the lipid-soluble dye DiD; the difference between the red and green QDs reflects the greater spectral overlap between the emission of the red QDs and the absorbance of the dye. Unlike in previous studies using aqueous solutions,[17] there is no immediate, large QD quench that is non-FRET related. This probably reflects the lack of QD clumping and

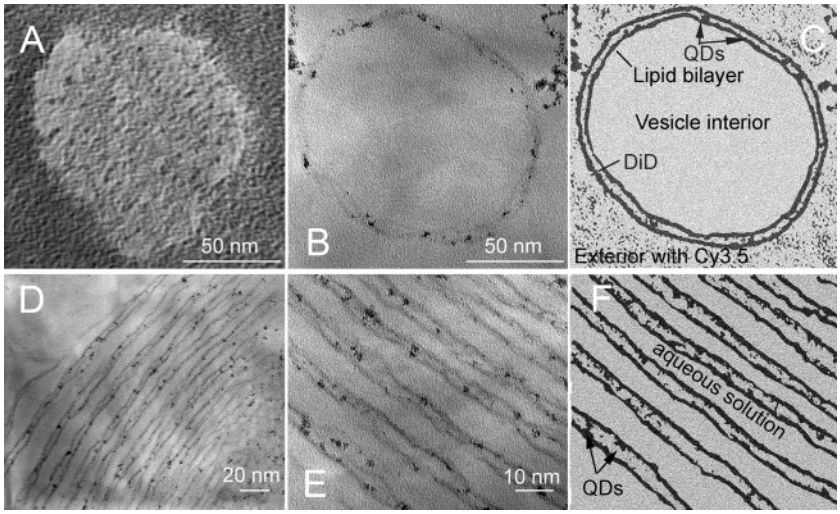

Figure 3. TEM images of whole and thin sectioned vesicles. (A) negatively stained whole vesicle at low resolution showing dark spots "peppered" over the surface. These spots are >30% each Cd and Se. (B) Thin section through a vesicle at the same magnification, showing dark areas associated with the lipid membrane. (C) Schematization of B showing the location of QDs within the lipid bilayer. The dye DiD also localizes within this layer; the vesicle is immersed in an aqueous external solution that may contain Cy3.5. (D) Thin section through a multilamellar vesicle, showing multiple layers of lipid, all of which contain QD material. (E) Closeup of D showing QD material concentrated within the lipid (narrower layers) rather than in the aqueous solution between the lamellae (wider layers). (F) Schematization of E showing the multiple layers of lipid (black lines) containing QD material in aggregates of various sizes.

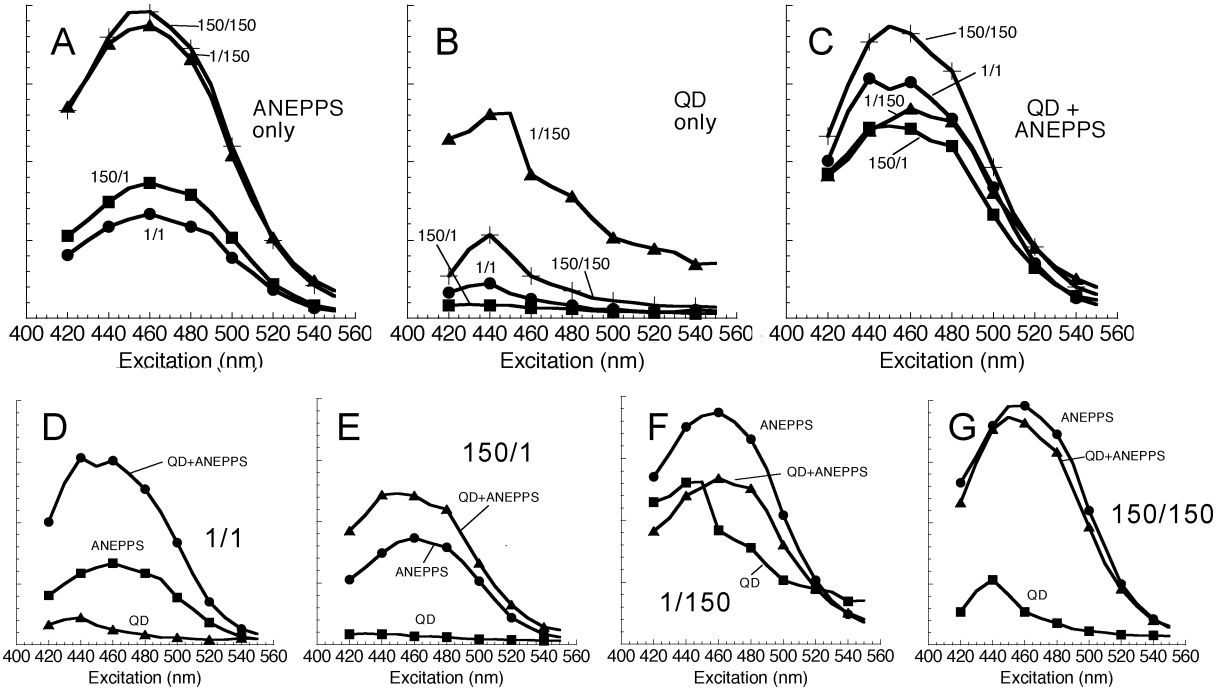

Figure 4. Excitation spectra at $\lambda_{Em} = 610$ nm of vesicles containing red QDs, ANEPPS, or both. The *y* axes are arbitrary units but relative strengths are preserved. Valinomycin is present, and the concentration of ANEPPS is 5 μM. QDs are highly diluted so that their typical absorbance peaks are not seen. (A−C) Spectra with low K^+ both inside and outside (1/1;●); high K_{in}/low K_{out} (150/1; ■); high K_{in}/high K_{out} (150/150,+); and low K_{in}/high K_{out} (1/150, ▲). (A) ANEPPS alone, (B) Red QD alone, and (C) Red QD + ANEPPS. (D−G) Comparison of spectra containing QDs alone (■), ANEPPS alone (●), and QD + ANEPPS (▲). (D) Low K^+ both inside and outside (1/1). **E**, High K_{in}/low K_{out} (150/1). F, Low K_{in}/high K_{out} (1/150). (F) High K_{in}/high K_{out} (150/150).

other nonspecific mechanisms that occur when the QDs float free but not when they are embedded in vesicles.

TEM Examination of Vesicles by Whole Mount and Thin Section. The relatively low values of FRET for Cy3.5, which are relatively independent of concentration, suggest that only a small fraction of the QDs in vesicles are accessible to this water-soluble dye. Similar results are seen with the Cy3.5 inside rather than outside the vesicles (data not shown), suggesting that most of the QDs are inside the lipid bilayer and do not contact the aqueous solution. To confirm this, we inspected the vesicles by TEM as whole mounts as well as embedded and sectioned into 50−100-nm-thick sections for TEM examination. The resulting images show dark particles, confirmed by EDS to consist of Cd and Se at an ~1:1 ratio, located primarily between vesicle leaflets (Figure 3).

Di-4-ANEPPS. For studies of energy transfer between QDs and di-4-ANEPPS, we prepared vesicles that contained high-K^+ and low-K^+ solutions and were dissolved in either high K^+ solution, low K^+ solution, or a 50:50 mix for a total of six sets of vesicles (low K_{in}/low K_{out}, high K_{in}/high K_{out}, low K_{in}/high

K_{out}, high K_{in}/low K_{out}, high K_{in}/50:50 K_{out}, and low K_{in}/50:50 K_{out}). In the absence of a charge carrier, the Nernst potential across the membrane of all of these vesicles is 0; however, if a K^+ ion channel is added to the membrane, then a potential is generated according to the usual Gibbs free energy equation

$$V = \frac{RT}{F} \ln\left(\frac{K_{out}}{K_{in}}\right) \tag{3}$$

The K^+ channel used in these studies was the peptide antibiotic valinomycin. Although the $V = 0$ case, just before the addition of valinomycin, was used as a control, simply varying K^+ concentrations without charge separation is interesting in itself. In early work with styryl dyes, it was shown that they localize inside the membrane near the lipid/water interface nearest where they enter; it was thus expected that vesicles containing ANEPPS would be sensitive to external ionic concentrations as well as to transmembrane potential.[18,19]

We tested both ANEPPS and QDs for function as energy acceptors, beginning by an examination of the excitation spectra. At a wavelength where the acceptor emits but the donor does not, the magnitude of the excitation spectrum of the energy acceptor (*A*) can be determined by the expression $A = \epsilon_A + f\epsilon_D$, where f is the transfer efficiency and ϵ_A and ϵ_D are the extinction coefficients of the energy acceptor and donor.[20] When there is no FRET, the excitation spectrum is identical to the absorption spectrum of the energy acceptor.

The hypothesis that QDs could act as energy donors to ANEPPS was tested first. Both excitation and emission spectra were examined. The excitation spectra were taken with emission wavelengths beyond the red edge of the QD emission, 650 nm (for red QDs) and 635 nm (for green QDs). The results revealed no energy transfer: the excitation spectra were equivalent to those of ANEPPS alone. The spectra changed by <1% upon the addition of valinomycin (spectra available in Supporting Information).

The possibility of QDs behaving as acceptors was not eliminated; however, the broad absorbance of the QDs and the broad emission of ANEPPS made the deconvolution of the spectra difficult. For excitation scans, the emission wavelength was chosen to be the red QD emission peak at 610 nm. At this wavelength, vesicles containing ANEPPS alone excited efficiently and showed a strong K^+ dependence; the excitation peak was at least 2-fold higher when external K^+ was high, irrespective of voltage (Figure 4A). The QDs showed somewhat of a similar effect, with strongest excitation when both voltage and external K^+ were high (Figure 4B). It was notable that the exciton peak visible in the QD absorbance spectrum (Figure 1) did not appear on these excitation scans.

When both QD and ANEPPS were in vesicles, the difference between high and low external K^+ was greatly lessened, with moderate qualitative changes to the shape of the spectra (Figure 4C). Alternatively, this means that at the emission wavelength of 610 nm, there was a large difference between the excitation spectra of ANEPPS alone and QD + ANEPPS only when external K^+ was low (Figure 4D). When either internal or external K^+ was high, there was a moderate change to the ANEPPS spectrum when QDs were added, which could either be a spectral enhancement (Figure 4E) or a suppression (Figure 4F); however, when both internal and external K^+ were high, the absorbance of QD + ANEPPS was almost indistinguishable from that of ANEPPS alone (Figure 4G).

The most striking spectral differences between ANEPPS alone and QD + ANEPPS were seen with low K^+ both external and internal to the vesicles. Did this represent energy transfer? The differences between the excitation spectra of QD + ANEPPS and ANEPPS alone revealed at least two processes that were occurring. In the low K_{in}/low K_{out} case, the difference was a sum of QD excitation and ANEPPS excitation; that is, the presence of the QDs appeared to mitigate the reduction in ANEPPS excitation due to low K^+, returning the dye almost to its high K^+ performance. In addition, QDs did seem to act as energy acceptors to some extent, resulting in an increase in QD

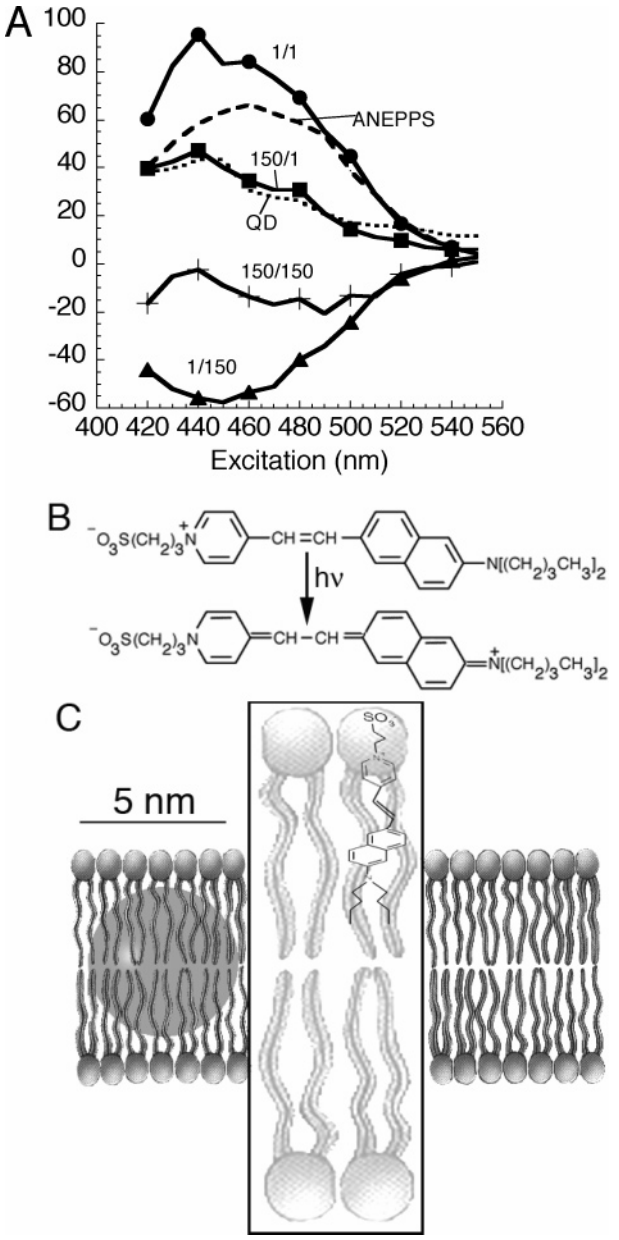

Figure 5. (A) Excitation spectral differences (*y* axis is arbitrarily scaled but included to show the position of 0) between vesicles with ANEPPS and red QDs and ANEPPS alone. $\lambda_{Em} = 610$ nm. Differences are shown for low K^+ both inside and outside (1/1;●); high K_{in}/low K_{out} (150/1; ■); high K_{in}/high K_{out} (150/150,+); and low K_{in}/high K_{out} (1/150, ▲). Shown for comparison are the excitation spectra of QDs only (-----) and ANEPPS only (− − −). (B) Structure of di-4-ANEPPS before (above) and after (below, *hν*) photoexcitation. (C) Believed orientation of ANEPPS binding to lipid bilayers[21] and presumed location of quantum dot. Shown are the polar headgroups (ovals) and hydrophobic tails (wavy lines) of the lipid bilayer; the approximate relative size and position of a hydrophobic QD (grey circle); and a blown-up image (center) showing ANEPPS binding to both the polar headgroup and hydrophobic tails.

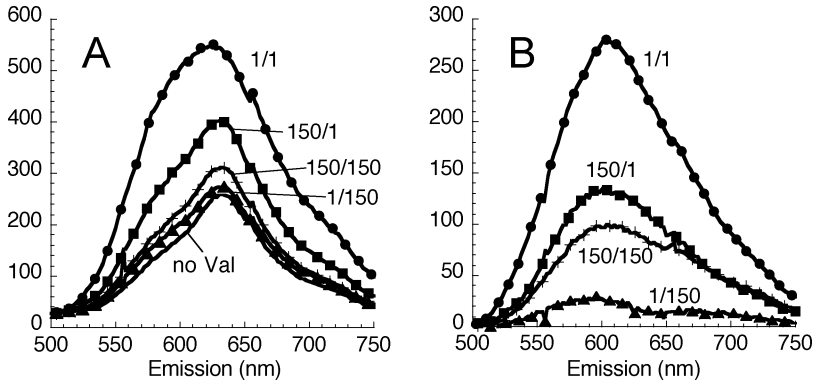

Figure 6. Emission spectra (λ_{Ex}=440 nm) of vesicles containing both red QDs and di-4-ANEPPS in solutions containing different values of internal and external K^+. The *y* axes are emission in arbitrary units with numbers included to permit comparison. The traces shown are averages of three independent experiments with error bars smaller than the symbols; the numbers give K_{in}/K_{out} in mM. (A) In the absence of valinomycin, vesicles in osmotically balanced solutions with different values of K_{in}/K_{out} show the same emission peak (−−−, "no Val"). Upon valinomycin addition, the largest spectral change is seen in vesicles with low K^+ both inside and outside (1/1; ●); a smaller change in high K_{in}/low K_{out} (150/1; ■); a very small change in high K_{in}/high K_{out} (150/150,+); and no significant change in low K_{in}/high K_{out} (1/150, ▲). (B) Subtraction of the "no Val" background shows that the fluorescence change is broad and centered about 610 nm, or slightly bluer than the original QDs (original peak 620 nm).

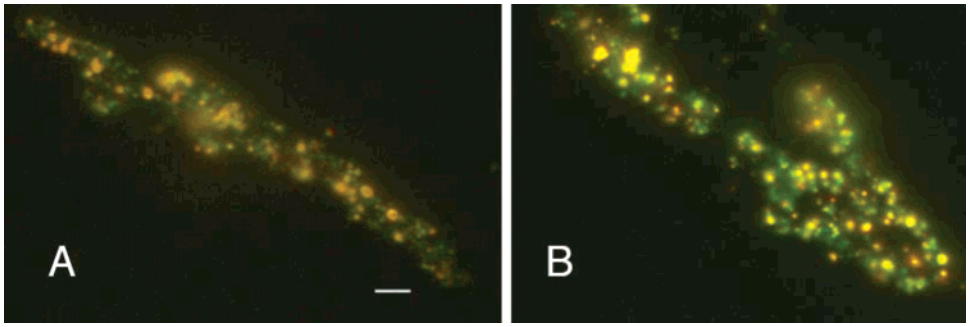

Figure 7. Fluorescent appearance of vesicles with red QD and 5 μM di-4-ANEPPS before and after valinomycin addition. Internal and external solutions are both 1 mM KCl. Scale bar=5 μm; epifluorescence with GFP filter. (A) Before valinomycin. (B) After valinomycin, showing increased fluorescent intensity and blue-shift. Images taken with identical gain and exposure times and unprocessed.

associated excitation; however, this effect was much smaller than that of ANEPPS enhancement. With high K_{in} and low K_{out}, only an increase in QD excitation was seen, with no apparent ANEPPS component. High K_{in}/high K_{out} appeared to be similar, but there was some degree of overall excitation suppression. In the low K_{in}/high K_{out} case, any possible QD component was swamped by a large ANEPPS suppression. All of the subtraction spectra are shown in Figure 5A, with the spectra of QD vesicles alone and ANEPPS alone included for comparison. Also shown is a schematic of ANEPPS binding to lipid bilayers that explains its different response to ions inside versus outside of the vesicle (Figure 5B and C).

It thus appeared that although the presence of ANEPPS may cause increased QD-associated excitation, the predominant feature of the spectra was a decrease in K^+ sensitivity of ANEPPS in the presence of QDs. Emission spectra and epifluorescence microscopy were performed to confirm or deny these observations. Because of the broad QD absorption, choosing a wavelength at which only di-4-ANEPPS was excited was not possible. Four wavelengths were investigated; three at which QDs excited efficiently and ANEPPS did not, 360, 400, and 530 nm, and one at which both excited efficiently, 440 nm. No significant changes with K^+ concentrations or valinomycin addition were seen at any excitation wavelength other than 440 nm. (See Supporting information for full negative spectra.)

At 440 nm excitation, vesicles with low K_{in}/low K_{out} exhibited visibly brighter fluorescence than any of the other vesicle preparations (Figure 5A). Interestingly, because the Nernst potential was 0 in this case, the effect was dependent upon the presence of valinomycin; in the absence of valinomycin, the emission spectra of all of the vesicle preparations were indistinguishable. Corresponding with the excitation spectra, the vesicles with high external K^+ showed weak or imperceptible changes when valinomycin was added (Figure 5B).

The observed spectral variations differed quantitatively and qualitatively from the classic voltage-related spectral changes of ANEPPS;[22] the latter were detectable by our fluorescence techniques but only represented an ∼5% shift in spectral peak (spectra not shown but are available in Supporting Information). Vesicles containing ANEPPS only did not change visually upon epifluorescence inspection when valinomycin was added, irrespective of the solutions inside or outside. In contrast, vesicles containing QD and ANEPPS in low K_{in}/low K_{out} demonstrated rapid visible brightening and spectral shift when valinomycin was added (Figure 7).

The excitation difference spectrum in Figure 5 seemed to imply that the spectral changes seen in low K_{in}/low K_{out} represented energy transfer to QDs as well as changes in efficiency of ANEPPS excitation. If this were the case, then the emission spectra should reflect the sum of ANEPPS and QD emission at varying intensities. In addition, the spectral changes seen should be dependent upon the concentrations of ANEPPS and QDs.

To test this hypothesis, we measured spectra across a 32-fold range of ANEPPS concentrations using low K_{in}/low K_{out} solutions only. At all ANEPPS concentrations, vesicles containing QD + ANEPPS were dimmer than those containing ANEPPS alone (Figure 8A). In addition, the spectrum in the

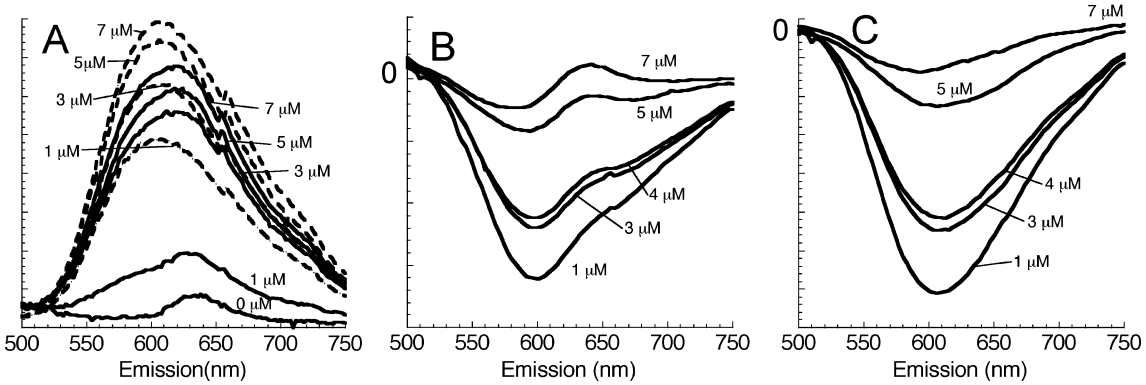

Figure 8. Spectra of vesicles containing QD + ANEPPS or ANEPPS alone, in the presence of valinomycin. The *y* axes give arbitrary units with the positions of the zeroes shown. (A) Concentrations of ANEPPS ranging from 0 to 7 μM for vesicles containing QDs (−−−, concentrations on right-hand side) or vesicles without QDs (− − −, concentrations on left-hand side). (B) Subtraction of the directly excited ANEPPS dye from the QD + ANEPPS vesicles shows a concentration-dependent quenching. The peak of the directly excited QDs is apparent (arrow). (C) Subtraction of the directly excited QD peak from panel B yields a broad peak centered about 605 nm.

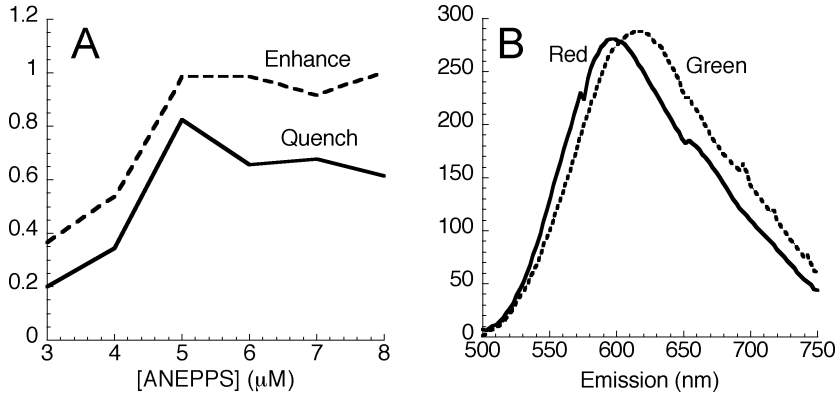

Figure 9. Spectral changes seen with QDs and ANEPPS in symmetric 1 mM KCl solution in the absence of valinomycin. (A) The enhancement of an "unknown" spectrum solved for using eq 4 (− − −) tracks the quenching of the emission of ANEPPS alone (−−−−) over a concentration range. (B) Appearance of the unknown spectrum for red QDs (original peak, 620 nm, −−−−) and green QDs (original peak, 570 nm, -------).

presence of QDs showed a significantly redder component than the dye alone, one that was not accounted for by direct QD excitation (Figure 8B and C).

The subtraction spectra of QD + ANEPPS shown in Figure 8C could not be fit to the ANEPPS spectrum alone; that is, the dimming of vesicles containing QDs was not due simply to quenching of ANEPPS. A reasonable fit could only be obtained by introducing an "unknown" spectrum and solving the equation

$$\text{Difference}(\lambda) = \alpha[ANEPPS] + \beta[U] \qquad (4)$$

where α, and β are amplitudes, [ANEPPS] represented the amount of ANEPPS quenching at a given concentration, and [U] represented the unknown spectrum. This provided a unique fit to Figure 8C with a fraction of the ANEPPS quenching ranging from 20−82% as the ANEPPS concentration rose. The unknown spectrum was enhanced as ANEPPS was quenched (Figure 9A).

The interpretation of the meaning of this unknown spectrum is not entirely known. However, the use of green QDs in a series of identical experiments yielded a solution for an unknown that was different that that obtained with red QDs (Figure 9B). Hence, it is likely that this enhanced spectrum reflects some form of energy transfer between QDs and ANEPPS. Relatively few studies have been performed with QDs as energy acceptors, where in most of these, the QDs were embedded in a thin polymer film. Energy transfer was attributed both to dipole−dipole Förster mechanisms[23] and to exciton diffusion;[24] in the latter case, unexplained spectral shifts were also seen. However, it is possible that the phenomena we observe are not due to energy transfer, but to changes in ionic concentration around the QDs and ANEPPS molecules. Future work will attempt to explain the observed steady-state spectra using time-resolved spectroscopy.

Conclusions

We have demonstrated that efficient FRET occurs between QDs embedded in vesicles and a lipid-soluble dye (DiD). Less efficient but nonnegligible FRET was found to take place from the fraction of the embedded QDs that are sufficiently close to the aqueous solution to a water-soluble dye, Cy 3.5. Leakage of vesicles is not seen over a time course of several hours. This work opens the way toward using QDs within the membrane leaflets of biological cells, where they may act as FRET donors either to naturally occurring molecules (e.g., proteins), to genetically engineered constructs (e.g., proteins linked to a fluorescent protein), or to organic dyes added to the membrane or to the inside or outside of the cell.

A critical feature of biological cells is the large transmembrane potential. Two questions needed to be addressed. The first, does the spectrum of QDs subject to this potential change significantly? This we were able to answer in the negative. This is not surprising, for although QDs demonstrate a remarkably large Stark shift in comparison with the bulk material, its visualization in ensembles of QDs has been complicated by inhomogeneous spectral broadening. This led to early controversy regarding structure of the QD ground state and whether

it possessed a permanent dipole moment (leading to a first-order Stark effect) or was polarizable (second-order effect).[25−27] Only measurements from single QDs have succeeded in confirming the Stark effect, which turns out to have components of both first and second order.[28]

The second question, can the properties of QDs be exploited to create a voltage-sensitive probe or to improve the properties of existing probes?, has been addressed but not fully answered. Intriguing spectral changes are seen with QDs in vesicles and the voltage-sensitive dye di-4-ANEPPS. Energy transfer occurs between the QDs and the dye in the presence of valinomycin, presumably with the dye acting as a donor and the QDs acting as acceptors; however, the spectrum that is enhanced with ANEPPS quenching is shifted from the original QD spectrum. The direction of the shift, but not its magnitude, is dependent upon the spectrum of the original QDs.

The mechanisms behind this change are unknown, and the overlap of spectra makes confirmation of energy-transfer processes difficult; however, we were able to establish several facts. First, the magnitude of the spectral shift with valinomycin addition is dependent not upon membrane potential, but KCl concentration. Negligible changes are seen upon valinomycin addition to vesicles in high K^+ (150 mM) external solution.

Excitation spectra are able to eliminate ANEPPS behaving as an energy acceptor because, at wavelengths at which ANEPPS emits but QDs do not, the excitation spectra are simply equivalent to those of ANEPPS. However, at a wavelength at which both emit, excitation spectra are seen that are consistent with the observed changes in emission. Low external K^+ efficiently suppresses ANEPPS excitation, and addition of QDs removes this suppression. This results in a series of spectra that change qualitatively based upon K^+ concentration.

If in fact QDs are acting as energy acceptors, then the explanation for their shifted and broadened spectrum is unknown. Other work in progress includes experiments with QDs that are able to act as donors to ANEPPS (i.e., blue-emitting QDs) and with ionophores that conduct ions other than K^+. However, these preliminary data suggest an important potential use of QDs in the design of ion-selective chromophores.

Acknowledgment. J.K. and J.N. acknowledge that this material is based upon work performed at the Jet Propulsion Laboratory, California Institute of Technology, supported by a contract with the National Aeronautics and Space Administration. N.C. wishes to acknowledge support from the Nuffield Foundation, NUF-NAL. We thank Randall Mielke for the TEM images.

Supporting Information Available: Full negative spectral data and emission spectra at 360- and 530-nm excitation. This material is available free of charge via the Internet at http://pubs.acs.org.

References and Notes

(1) Mamedova, N. N.; Kotov, N. A.; Rogach, A. L.; Studer, J. *Nano Lett.* **2001**, *1*, 281.
(2) Medintz, I. L.; Clapp, A. R.; Mattoussi, H.; Goldman, E. R.; Fisher, B.; Mauro, J. M. *Nat. Mater* **2003**, *2*, 630.
(3) Wang, S. P.; Mamedova, N.; Kotov, N. A.; Chen, W.; Studer, J. *Nano Lett.* **2002**, *2*, 817.
(4) El Maarouf, A.; Rutishauser, U. *J. Comp. Neurol.* **2003**, *460*, 203.
(5) Maffei, A.; Prestori, F.; Rossi, P.; Taglietti, V.; D'Angelo, E. *J.Neurophysiol.* **2002**, *88*, 627.
(6) Meers, P.; Ali, S.; Erukulla, R.; Janoff, A. S. *Biochim. Biophys. Acta* **2000**, *1467*, 227.
(7) Terasaki, M.; Miyake, K.; McNeil, P. L. *J. Cell Biol.* **1997**, *139*, 63.
(8) Tominaga, T.; Tominaga, Y.; Ichikawa, M. *Pflugers Arch.* **2001**, *443*, 317.
(9) Millard, A. C.; Jin, L.; Lewis, A.; Loew, L. M. *Optics Lett.* **2003**, *28*, 1221.
(10) Wong, M. S.; Stucky, G. D. *Abstracts of Papers of the American Chemical Society* **2001**, *221*, U572.
(11) Kloepfer, J. A.; Mielke, R. E.; Wong, M. S.; Nealson, K. H.; Stucky, G.; Nadeau, J. L. *Appl. Environ. Microbiol.* **2003**, *69*, 4205.
(12) Dabbousi, B. O.; RodriguezViejo, J.; Mikulec, F. V.; Heine, J. R.; Mattoussi, H.; Ober, R.; Jensen, K. F.; Bawendi, M. G. *J. Phys. Chem. B* **1997**, *101*, 9463.
(13) Zhang, C. X.; O'Brien, S.; Balogh, L. *J. Phys. Chem. B* **2002**, *106*, 10316.
(14) Lakowicz, J. R. *Principles of Fluorescence Spectroscopy*, 2nd ed.; Kluwer Academic: New York, 1999.
(15) Schmelz, O.; Mews, A.; Basche, T.; Herrmann, A.; Mullen, K. *Langmuir* **2001**, *17*, 2861.
(16) Hashimoto, F.; Tsukahara, S.; Watarai, H. *Langmuir* **2003**, *19*, 4197.
(17) Willard, D. M.; Carillo, L. L.; Jung, J.; Van Orden, A. *Nano Lett.* **2001**, *1*, 469.
(18) Fluhler, E.; Burnham, V. G.; Loew, L. M. *Biochemistry* **1985**, *24*, 5749.
(19) Loew, L. M.; Simpson, L. *Biophys. J.* **1981**, *34*, 353.
(20) Weber, G.; Teale, F. W. J. *Trans Faraday Soc.* **1958**, *54*, 640−648.
(21) Loew, L. M. *Pure Appl. Chem.* **1996**, *68*, 1405.
(22) Fromherz, P.; Lambacher, A. *Biochim. Biophys. Acta* **1991**, *1068*, 149.
(23) Javier, A.; Yun, C. S.; Sorena, J.; Strouse, G. F. *J. Phys. Chem. B* **2003**, *107*, 435.
(24) Sirota, M.; Minkin, E.; Lifshitz, E.; Hensel, V.; Lahav, M. *J. Phys. Chem. B* **2001**, *105*, 6792.
(25) Sacra, A.; Norris, D. J.; Murray, C. B.; Bawendi, M. G. *J. Chem. Phys.* **1995**, *103*, 5236.
(26) Colvin, V. L.; Alivisatos, A. P. *J. Chem. Phys.* **1992**, *97*, 730.
(27) Colvin, V. L.; Cunningham, K. L.; Alivisatos, A. P. *J. Chem. Phys.* **1994**, *101*, 7122.
(28) Empedocles, S. A.; Bawendi, M. G. *Science* **1997**, *278*, 2114.